Loss of coherence in cavity-polariton condensates: effect of disorder vs. exciton reservoir.

A. A. Demenev, Ya. V. Grishina, S. I. Novikov, and V. D. Kulakovskii
Institute of Solid State Physics, RAS, Chernogolovka, 142432 Russia

C. Schneider and S. Höfling
Technische Physik, Physikalisches Institut and Wilhelm Conrad Röntgen Research Center for Complex Material Systems, Universität Würzburg , D-97074 Würzburg, Germany

Time evolution of long-range spatial coherence in a freely decaying cavity-polariton condensate excited resonantly in a high-Q GaAs microcavity (MC) is found to be qualitatively different from that in nonresonantly excited condensates. The first-order spatial correlation function $g^{(1)}(r_1, r_2)$ in response to resonant 1.5 ps pump pulses at normal incidence leaving the exciton reservoir empty is found to be nearly independent of the excitation density. $g^{(1)}$ exceeds 0.7 within the excited spot and decreases very slowly in the decaying and expanding condensate. It remains above 0.5 until the polariton blueshift $\alpha|\psi^2|$ gets comparable to the characteristic amplitude of the disorder potential δE_{LP}. The disorder is found to reveal itself at $\alpha|\psi^2| \lesssim \delta E_{LP}$ in fast and short-range phase fluctuations as well as vortex formation. They lead to oscillations in $g^{(1)}(t)$, but have little effect on the overall coherence, which is well reproduced in the framework of the Gross-Pitaevskii equations.

I. INTRODUCTION

Spatial coherence at large distances is the basis of the quantum behavior of different systems demonstrating superconductivity and superfluidity. It was extensively studied in conventional superconductors. The realization of Bose-Einstein condensation in a gas of ultracold atoms opened up the possibility to investigate the dynamics of spatial coherence during condensate formation and decay.[1] The studies of condensation in a gas of ultracold atoms showed that the coherence in this gas expands with a constant velocity of about 0.1 mm/s.[2]

Much more favorable conditions for studying the dynamics of the spatial coherence in boson systems were created by the implementation of macrooccupied states in exciton-polariton systems in semiconductor microcavities (MC).[3–5] Exciton polaritons are bosonic quasiparticles formed in the regime of the strong interaction of MC photons and excitons in quantum wells in the active MC region. From the exciton component they inherited a nontrivial interparticle interaction. A very small, $< 10^{-4} m_e$, (m_e being the free electron mass), effective mass inherited from the photonic component provides a sufficiently high condensation temperature. Besides, the photonic component makes it possible to directly study the properties of the polariton system. As a consequence, the dynamics of coherence in exciton-polariton systems can be investigated by time-resolved measurements of the first order correlation function $g^{(1)}$ of their radiation.

In the recent studies of macrooccupied polariton states in MCs an array of spectacular phenomena was discovered which are characteristic of Bose-Einstein condensates (BEC), such as superfluidity[6], quantized vortices[7], quenching of the Zeeman splitting[8], Josephson effect[9], and others that enable to refer to this system as a "dynamic" BEC. It should be noted, however, that, in contrast to conventional superconducting and superfluid systems, the exciton-polariton system is highly nonequilibrium due to the very short lifetime of polaritons, which brings peculiarities in its properties.

By now most studies of polariton condensate coherence have been carried out using interband photoexcitation that generates hot electrons and holes in quantum wells.[10–17] They bound into long-lived excitons forming a so-called exciton reservoir. Condensate formation occurs as a result of scattering of excitons in low polariton (LP) states with small lateral wavevectors, k, which assumes a stimulated character at a critical polariton density and leads to formation of a dynamic condensate at $k = 0$. The spatial coherence in the LP condensate was found to expand with a velocity of $\sim 10^8$ cm/s[16], which is many orders of magnitude higher than in a gas of ultracold atoms. At the same time, the coherence length L_c in the investigated nonresonantly excited LP condensates does not exceed several tens μm. The main reasons for condensate decoherence besides limited LP lifetime are the potential disorder and interaction with the exciton reservoir.[18]

The disorder can lead to formation of a Bose-glass insulating phase in which disconnected LP condensates in different regions become phase-locked.[19–21] The nonequilibrium character of the processes occurring in the LP system in a disorder potential can lead to an exotic quantum phase transition of the Berezinskii-Kosterlitz-Thouless type.[22,23] $g^{(1)}(\Delta r)$ in this regime was found to decay by a power law, the exponent being dependent on the number of modes in the condensate.[11,24,25]

One might expect a higher spatial coherence of the LP condensate arising from optical parametric oscillations (OPO) under resonant excitation near the inflection point of the LP dispersion as in this case direct stimulated scattering from the driven coherent mode is one of the main sources of LPs in the condensate.[5] However, spatial coherence was found to differ only slightly from

that reached in the case of above band gap excitation[26], which seems to be connected with an effective filling of the exciton reservoir in the OPO process.

In the present paper we address time evolution of a lateral coherence in a freely decaying LP condensate system with an empty exciton reservoir. For this purpose the condensate is excited resonantly with 1.5 ps-long pulses at $k = 0$ in a high Q MC with polariton lifetime $\tau_{LP} \sim 20$ ps. The behavior of $g^{(1)}(t)$ is found to differ qualitatively from that in nonresonantly excited condensates.

The laser pulses set up the high spatial coherence of the condensate with high $g^{(1)}(r_1; r_2)$ exceeding 0.7 and nearly independent of pump power. The coherence inherited from the laser pulses is found to decrease in the decaying condensate very slowly, by less than 10% during 80 ps. When the LP-LP interaction energy becomes comparable with the amplitude of potential fluctuations the redistribution of flows in the condensate expanding in the disordered potential leads mainly to short time oscillations in $g^{(1)}$ indicating the conservation of the overall condensate coherence. Experimental findings are well reproduced within the framework of Gross-Pitaevskii equations when both the limited size of the pumped spot, the gradient polariton energy in the MC, and disorder are taken into account.

This manuscript is structured as follows. In Sec. II the samples in question and the experimental techniques are described. The presentation of the experimental studies of time evolution of LP condensate in real and momentum spaces and its long range spatial coherence in Sec. III is followed by the discussion based on the Gross-Pitaevskii equations. Finally, a conclusion is given in Sec. IV.

II. EXPERIMENTAL DETAILS

We studied a $\lambda/2$ GaAs/AlAs MC structure grown by molecular beam epitaxy on a GaAs substrate and already investigated in our previous works[28–30]. The active layer contained four 7 nm thick GaAs quantum wells separated by 4 nm thick AlAs barriers and located at the central antinodes of the electric field. The lower (upper) Bragg reflector consisted of 32 (for the top mirror) and 36 (for the bottom mirror) AlAs and $Al_{0.13}Ga_{0.87}As$ pairs. The quality factor of the MC reached (3–5)x10^4 and the Rabi splitting was 10.5 meV. The experiments were performed at $T \approx 10$ K.

The investigation of LP emission was carried out in a transmission geometry from the back side of the sample to avoid any contribution from the scattered laser beam. With this purpose the GaAs substrate was locally ($\sim$ 300x700 μm) removed with the use of citric acid/hydrogen peroxide selective etching (AlAs in the nearest mirror served as an etch stop layer). The MC layer in the etched area was slightly strained, which caused lowering of the lateral symmetry and, as a consequence, a slight splitting of the LP states varying in the etched area in a range of 30 - 140 μeV.[31]

Resonant excitation was performed by a mode-locked Ti-sapphire laser generating a periodic (f = 80 MHz) train of 1.5-ps-long pulses at $\hbar\omega_p = E_{LP}(k = 0) + 0.3$ meV. The sample was pumped at the normal to the MC plane. To avoid any excitation of the exciton reservoir we studied the MC with a negative detuning of the cavity and exciton modes $E_C - E_X \approx -6.5$ meV at $\mathbf{k} = 0$. It was determined from the transmission spectra measured in a linear regime. Above band gap excitation of the LP system was carried out with a laser pulse duration of 80 ps in the spectral range of the first reflection minimum. In both cases the laser beam was focused in a spot with diameter of 40 μm on the sample surface.

The dynamics of the LP emission intensity was detected using a streak camera with a time resolution of 3 ps. The emission spectra were measured with a spectral resolution of 0.2 meV, which limited the time resolution by $\sim$ 10 ps. To measure the distribution of the LPs in the k-space an additional lens was used in the optical system, which allowed collection of the radiation emerging from the MC at a certain angle Θ to its normal ($k = \omega sin\Theta/c$) and a certain point of the streak camera. That enabled us to record the LP distribution in the k-space with a time resolution of 3 ps.

The first order spatial coherence function characterizing the ability of the polariton system to interfere[32,33] is related to the off-diagonal elements of density matrix $\rho(\mathbf{r}_1, \mathbf{r}_2)$ in the coordinate space.

$$g^{(1)}(\mathbf{r}_1, \mathbf{r}_2) = \rho(\mathbf{r}_1, \mathbf{r}_2)/\sqrt{\rho(\mathbf{r}_1, \mathbf{r}_1)\rho(\mathbf{r}_2, \mathbf{r}_2)} \qquad (1)$$

To find $g^{(1)}$ we measured the interference of the light emitted from different points on the sample, since the amplitude and phase of the electric field of the cavity emission is directly proportional to those of the LP condensate wavefunction ψ.[10] The interferogram was measured with the use of a Michelson interferometer in a mode that ensured overlay of direct and mirror images. The overlay was obtained by passing a parallel beam of light through the Michelson interferometer, one arm of which is a reflective prism ensuring overlay of the original image on the reflected one with respect to the vertical axis. The path difference between the two rays was regulated by a delay line. The two light beams passing through the interferometer were collected at the detector of the streak camera located in the lens focus.

The space distribution of light intensity at the detector, $I_d(x)$, is given by $I_d(x) = I_1(x) + I_2(-x) + 2\sqrt{I_1 I_2}g^{(1)}(x; -x)cos[4\pi/\lambda(D_0 x/L_{od} + \delta l) + \phi_i]$ where $I_{1,2}$, δl and ϕ_i are the light intensities, the differences in the path lengths and phases in two interferometer arms, respectively, D_0 is the distance between the light beams, and L_{od} is the distance between the collective objective and detector. $g^{(1)}(x, -x)$ were extracted from the interferograms recorded for the set of δl with the step of $\lambda/8$.

III. EXPERIMENTAL RESULTS AND DISCUSSION

A. Time evolution of resonantly excited LP condensate in real and momentum spaces

The long, ~ 20 ps, LP lifetime τ_{LP} allowed investigating the coherence properties of the "pure" LP system, because resonance excitation with 1.5-ps long pulses almost didn't stimulated the exciton reservoir with energy $E \sim E_X = E_{LP}(k=0) + 9$ meV for our experimental temperature and timescale.

The time behavior of spatial coherence is investigated in a single-component LP system in a slightly laterally strained MC with the LP level split into two sublevels with orthogonal linear polarizations $E_{LP,x}$ and $E_{LP,y}$ ($E_{LP,x} - E_{LP,y} \sim 0.07$ meV). The LP system is generated in the ground linearly (π_y) polarized state by picosecond π_y polarized pulses. The linear polarization is maintained during condensate decay. The stability of the condensate polarization is qualitatively explained by a larger blueshift of the unexcited split off LP sublevel with a perpendicular linear polarization due to the fact that the repulsive interaction between LPs with the same linear polarization is smaller than between cross-polarized ones.

Note that the generation of LPs by picosecond pulses with any other polarization leads to the filling of both spin components. In the case of the circularly polarized pulses, one deals with a direct excitation of two components as their splitting (~ 0.1 meV) is less than the spectral width of the picosecond pulses (~ 1.5 meV). In the case of excitation of the split off pi_x- polarized LP states with π_x -polarized pulses, the filling of the lower π_y sublevel is activated by effective parametric scattering from the split off state taking place with conservation of both energy and momentum. The beating of two coherent spin components with different energies leads to oscillations of polarization in the decaying spinor condensate (so called inner Josephson effect[34]) that is well observed in the experiment.

Figures 1a and 2a show the typical time dependences of the spatial distribution of LP emission intensity $I(x,t)$. They were measured at the MC sites denoted as #1 and #2, respectively, with nearly the same negative detuning of $E_C - E_X = -6.4$ and -6.5 meV, respectively, under excitation $\hbar\omega_p = E_{LP}(k=0) + 0.3$ meV with $P \sim 0.12$ nJ/pulse. The emission was recorded from the central strip with a width of 4 μm. The blue shift of the LP emission line was ~ 0.4 meV.

In Figs.1a and 2a it is seen that $I(x)$ in the excited condensate ($t \sim 3$ ps) fluctuates along the strip. We connect these fluctuations with disorder. The much lower amplitude of the fluctuations of $I(x)$ in Fig.1a enables to conclude that the disorder at site #1 is markedly smaller. At $t > 3$ ps $I(x)$ decreases due to polariton leakage through the mirrors and broadens due to the condensate expansion caused by the repulsion LP-LP interaction.

Figures 3a and b show time dependencies $I(x)$ at the

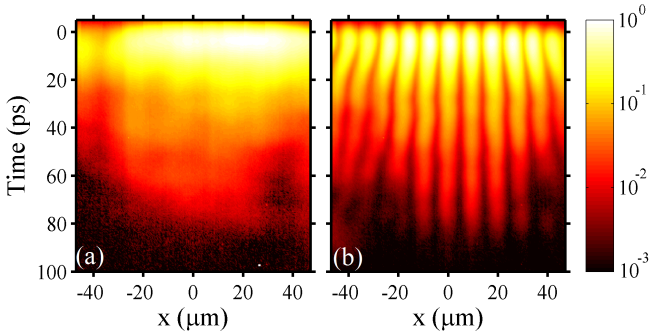

FIG. 1. (Color online) Time dependence of (a) spatial distribution of emission intensity of the LP condensate mode excited resonantly with 1.5-ps long pulses and (b) interferogram of its direct and mirror images measured with the use of a Michelson interferometer at #1. The spatial and time resolutions are 2 μm and 3 ps, respectively. $P = 0.12$ nJ/pulse.

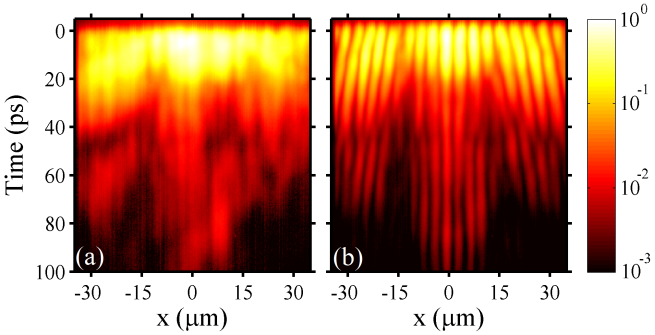

FIG. 2. (Color online) Time dependence of (a) spatial distribution of emission intensity of the LP condensate mode excited resonantly with 1.5-ps long pulses and (b) interferogram of its direct and mirror images at #2. $P = 0.15$ nJ/pulse.

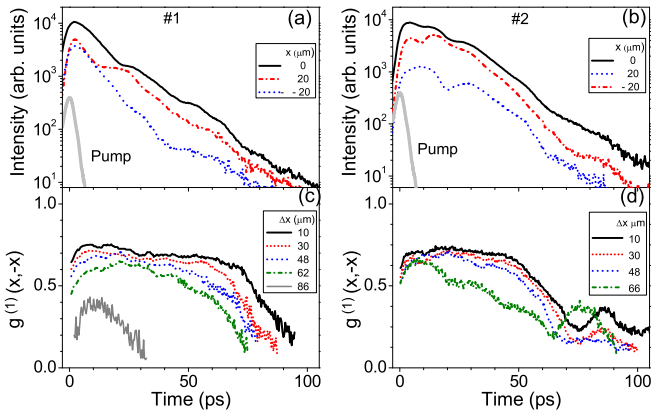

FIG. 3. (Color online) Time dependences of $I(x_i)$ from the center of the excited spot ($x_i = 0$) and its edges ($x_i = \pm 20$ μm) in #1 (a) and #2 (b). The pulse profile is shown by the gray solid line. Figures (c) and (d) show time dependences of $g^{(1)}(x,-x)$ at several values of Δx for the condensates in #1 and #2, respectively. The dependences were determined from the interferograms recorded with the same fringe period $T_{fr} = 7.5$ μm.

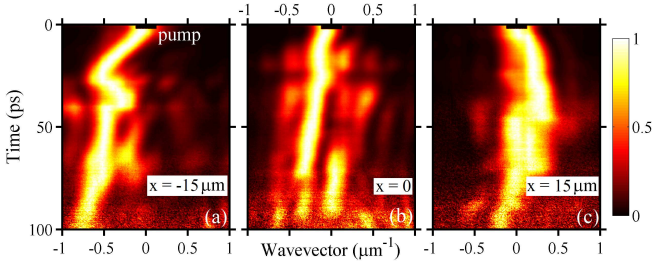

FIG. 4. (Color online) Time evolutions of $k-$distributions of LPs in the condensate in #2 at $x = -15$ (a), 0 (b), and $+15$ μm (c) measured with a spatial resolution of 14 μm (the k-resolution is 0.06 μm). For convenience, the dependences $I(k_x, t)$ are normalized to 1 at each time moment.

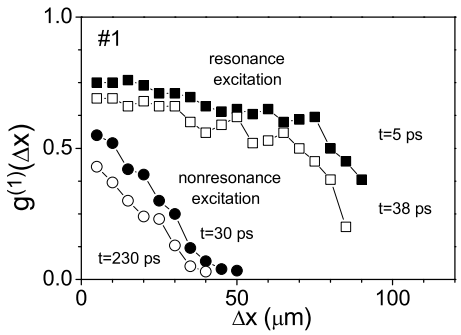

FIG. 5. (Color online) Dependences of $g^{(1)}(\Delta x)$ in #1 in the case of resonant (squares) and above band gap (circles) excitations. The dependences correspond to the delay times when L_c is maximal (solid points) and when the condensate density decreases by 10 -fold (open points).

center ($x = 0$) and edges ($x = \pm 20$ μm) of the excited spot for #1 and #2, respectively. $I(x = 0, t)$ decreases upon termination of the pump pulse as expected in the absence of an occupied exciton reservoir. The difference in the decay times in #1 and #2 ($\tau \approx 15$ and 19 ps, respectively) is related to a small variation of the cavity Q-factor along the MC in the area with an etched substrate.

The difference in $I(t)$ at $x = \pm 20$ μm is due to the asymmetry in the condensate expansion caused by the gradient of E_{LP} in the x-direction and disorder in the MC. They are also responsible for a strong difference in the k-distributions of the LPs in the center of the excited spot and its edges. This is illustrated in Fig. 4 displaying the time evolution of $I(k_x)$ in #2 at $x = 0$ and ± 15 μm with a spatial resolution of 14 μm (the k resolution is 0.06 μm^{-1}). For convenience, these dependences are normalized to 1 at each time moment.

Figure 4 shows that $I(k_x)$ at $x = 0$ and ± 15 μm coincide with each other only at $t \lesssim 3$ ps. The full width at half maximum (FWHM) of $I(k_x)$, $\Delta k(t < 3$ ps$)$=0.18 μm^{-1} corresponds to the pump pulse aperture of $\sim 1.5^o$. In the decaying condensate, the peak of $I(k_x)$ shifts with a nearly constant velocity $dk_{x,max}/dt \sim 40$ cm^{-1}/ps during ~ 40 ps, which allows explaining the shift of $k_{x,max}$ by the effect of the gradient of $E_{LP}(x)$ in the MC. The movement of the condensate at $x = \pm 15$ μm is additionally affected by an LP-LP repulsion. This effect dominates at small t (large n_c): Fig. 4 shows that at $t < 15$ ps the values of k_x at $x = 15$ and -15 μm have opposite signs. Experiments with various P showed that the difference between $dk_{x,max}/dt$ at $x = \pm 15$ and 0 μm decreases from ~ 140 cm^{-1}/ps at $P = 0.2$ nJ/pulse to ~ 60 cm^{-1}/ps at $P = 0.03$ nJ/pulse.

The monotonous variation of $k_{x,max}(x_i)$ is disturbed with increasing t. Figure 4 shows that at $x_i = \pm 15$ μm it occurs already at $t \sim 20$ ps whereas a jump in $k_{x,max}$ at $x = 0$ is observed only at $t \sim 50$ ps. The disturbance of the monotonous variation of $k_{x,max}(x_i)$ has to be connected to the redistribution of the condensate flows caused by the occurrence of disorder when the blue shift $\alpha|\psi(x)|^2$ decreases and becomes comparable with the amplitude of E_{LP} fluctuations. Here α is the constant of LP-LP interaction. Finally, note that Fig. 4 shows that the fluctuations in the FWHM of $I(k_x)$ are small and short. This behavior of Δk indicates that the condensate coherence inherited from the coherent pump is weakly influenced by redistribution of flows in different parts of the condensate.

B. Time evolution of long-range spatial coherence in the condensate.

Quantitative information about $g^{(1)}(\Delta x, t)$ was obtained from the studies of the time dependences of the interferograms of condensate emission registered with the use of the Michelson interferometer. Figure 1c shows that the interferogram of the emission from #1 at $P = 0.12$ nJ/pulse measured with spatial resolution of 2 μm demonstrates a highly pronounced interference. The dependences of $g^{(1)}(x, -x)$ extracted from the set of the interferograms measured with different delays between the direct and mirror images are shown in Figs. 3c for several $\Delta x = 2|x|$ smaller and larger than $d = 40$ μm. It is seen that $g^{(1)}$ at $\Delta x \lesssim d$ reaches ~ 0.73, which is close to the limited value of 0.87 when the interferogram is measured with fringe period T_{fr} of 7.5 μm and spatial resolution δ_x of 2 μm.

It is seen in Fig. 3c that in the decaying condensate, $g^{(1)}$ decreases very slowly. At $\Delta x < d$ it decreases by less than 10% when n_c decreases by nearly two orders of magnitude. Figure 3c also shows that $g^{(1)}(x, -x)$ remains large in the expanding condensate at $x > d/2$. So, $g^{(1)}(1.5d) \approx 0.6$ at $t = 10$ ps and decreases by less than 25% during the next 50 ps. Comparison of the dependences $g^{(1)}(x, -x)$ on Δx at $t = 5$ ps (n_c is close to its maximum) and at $t = 38$ ps (n_c decreases 10-fold) in Fig. 5 shows that in both cases $g^{(1)}$ depends weakly on Δx at $\Delta x \lesssim 1.5d$, the coherence lengths L_c determined using relation $g^{(1)}(L_c) = 1/e$ are ~ 90 and 80 μm at $t = 5$ and 38 ps, respectively.

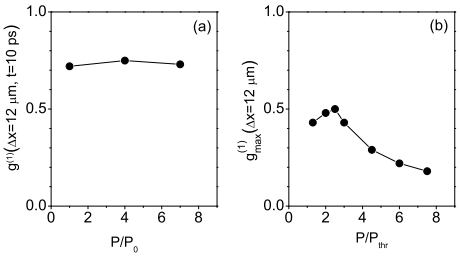

FIG. 6. (a) Dependence of $g^{(1)}(\Delta x = 12)$ μm on P in the resonantly excited condensate in the sample #1. The values of $g^{(1)}$ are measured at $t = 10$ ps, $P_0 = 0.03$ nJ/pulse. (b) Dependence of maximal values of $g^{(1)}(\Delta x = 12)$ μm on P in the nonresonantly excited condensate in the sample #1. P_{thr} is the threshold excitation density for condensation of LPs.

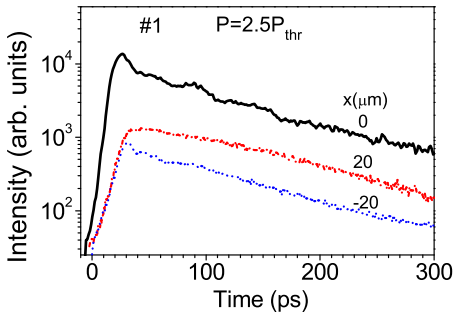

FIG. 7. (Color online) Time dependences of $I(x_i)$ recorded under the above band gap excitation at $P = 2.5P_{thr}$ from the center of the excited spot ($x_i = 0$) and its edges ($x_i = \pm 20$ μm). The pulse profile is shown by a gray solid line.

Finally, note that the magnitude of $g^{(1)}$ in the resonantly excited condensate depends very weakly on the excitation density. That is illustrated in Fig. 6a displaying the dependence of $g^{(1)}(\Delta x = 12)$ μm on P at $t = 10$ ps in a wide range of excitation densities from 0.03 to 0.2 nJ/pulse.

The effect of disorder is illustrated in Fig. 2b displaying the interferogram for #2. The interferogram shows that the disorder involves the appearance of local short time fluctuations in T_{fr}, marked smearing of fringes, and even their fork-like behavior. The time fluctuations in T_{fr} indicate the occurrence of those in the condensate phase $\phi(\mathbf{r}, t) = \omega^*_{LP}(\mathbf{r}, t)t - \mathbf{k}(\mathbf{r}, t)\mathbf{r} + \phi(t = 0)$.

The fluctuations of ϕ are caused by the redistribution of polariton flows in the condensate expanding in the disorder potential. This conclusion is supported by the observation of fluctuations in the angular distribution of condensate emission presented in Fig. 4. The fork-like behavior of the fringes at $t > 30$ ps is indicative of vortex formation in the expanding condensate.

The $g^{(1)}(t)$ dependences for #2 at several Δx less and larger than d are shown in Fig. 3d. Comparison of $g^{(1)}(t)$ in #1 and #2 in Fig. 3 shows that at $x \lesssim 50$ μm they only slightly differ from each other at $t \lesssim 50$ ps in spite of the fact that pronounced fluctuations in T_{fr} in #2 appear already at $t \sim 25$ ps. The effect of disorder on $g^{(1)}$ becomes pronounced only at $t \gtrsim 55$ ps when n_c decreases more than 30 times. Underline that the decrease of $g^{(1)}(t)$ at large t in #2 is not monotonous, it is followed by an oscillation, which indicates that the minima in $g^{(1)}(t)$ are mainly due to the local fluctuations in the condensate phase connected to the redistribution of flows in the condensate expanding in the disordered potential $\phi(x, t)$.

Thus, the experiments show that the resonantly excited condensate demonstrates the unique behavior of the long-range spatial coherence that differs qualitatively from observed earlier in nonresonantly excited MCs[16,18]. To directly compare the coherent properties of the resonantly and nonresonantly excited condensates we investigated them in the same MC in the range of small potential fluctuations.

Nonresonant excitation was carried out with 80-ps-long pulses at the first Bragg mirror reflection minimum. As in the earlier studies[16–18] we found that L_c is strongly dependent on P. Figure 6b shows that $g^{(1)}(\Delta x = 12$ μm reaches its maximum at $P \sim 2.5P_{thr}$ and than decreases gradually. Figure 7 shows the experimental dependences $I(x = x_i, t)$ and $g^{(1)}(\Delta x, t = t_i)$ obtained at $P \sim 2.5P_{thr}$ when the spatial coherence was maximal. The maximum n_c at this P is reached with a delay of about 20 ps relative to the pulse maximum. The long, ~ 100 ps, decay time of n_c is due to continuing condensation of polaritons from the exciton reservoir. The asymmetry in the dynamics of n_c at $x = \pm 20$ μm as well as under resonant excitation is connected to the gradient of $E_{LP}(x)$.

Figure 5 shows the experimental $g^{(1)}(\Delta x)$ dependences in the nonresonantly excited condensate at $t = 25$ ps when L_c is maximum (solid circles) and at $t = 220$ ps when n_c decreases by 10-fold (open circles) together with the corresponding $g^{(1)}(\Delta x)$ dependences in the resonantly excited condensate (solid and open squares, respectively). It is seen that $g^{(1)}$ in the nonresonantly excited condensate decreases rapidly with Δx. L_c at $t = 25$ ps is equal to 22 ± 2 μm, which is 4 times less than in the resonantly pumped condensate. The 10-fold decrease in n_c in the nonresonantly excited condensate is followed by a two-fold decrease in L_c whereas in the case of resonant excitation it is within $\sim 10\%$.

Thus, the high long-range coherence in the resonantly excited LP condensate is realized due to the empty exciton reservoir. The disturbance of the condensate coherence in the absence of an exciton reservoir can be caused by the LP-LP interaction, scattering by phonons (the experiment was carried out at 10 K)[27], and the disorder. The first two reasons are expected to result in a gradual variation in $g^{(1)}$ with increasing Δx at fixed t and with increasing t at fixed Δx.

The effect of disorder can be qualitatively different as it disturbs the radial expansion of the condensate caused by the repulsion interaction of LPs and leads to formation of condensate fluxes with $\mathbf{k}$-direction different from that

of **r**. The external fluxes getting into the strip cause fluctuations in n_c and **k** that are local in space and time. They are well seen in the experimental $I(x,t)$ and $I(k_x,t)$ dependences measured in #2 and shown in Figs. 3c and 4, respectively.

C. Numerical simulations of long-range spatial coherence in the condensate and discussion.

To estimate the effect of disorder on $g^{(1)}$ we have carried out simulations of time evolution of the condensate field with the use of a well-established model based on Gross-Pitaevskii equations with taking into account both the limited size of the pumped spot, the gradient of E_{LP}, and the disorder.[35–37].

The simulations were carried out with the use of parameters approximately corresponding to the experimental conditions: $d = 40$ μm, $\hbar\omega - E_{LP}(x=0) = 0.3$ meV, $dE_{LP}/dx = 2$ meV/mm, $dE_{LP}/dy = 0$, $\tau_{LP} = 30$ ps, the pulse duration $\tau = 1.5$ ps, and the pump beam aperture $\Delta\Theta = 1^o$. Figures 8 and 9 show the results of simulations of $I(x,t)$ and $\Delta\psi(x,t) = \psi(x,t) - \psi(0,t)$, respectively, in the strip $|y| < 2$ μm for MC with $\nabla E_{LP}(x) = const$ without and with disorder. Calculated time dependences of $k-$distribution of condensate emission from the center of excited spot and its edges are shown in Fig. 10.

Comparison of Figs. 1, 2 and 4 with Figs. 8 and 10 shows that the simulations taking into account nonzero ∇E_{LP} reproduce both an asymmetric expansion of the excited condensate and the difference in $k_m(t)$ at the center of the excited spot and its edges connected to the condensate expansion due to the repulsive polariton interaction and the movement of the entire condensate in the gradient of E_{LP}. Experimentally observed fluctuations of $I(x,t)$, fluctuations and/or jumps in $k_m(t)$, as well as the local short time blurring of the interferogram are reproduced qualitatively only when the disorder is taken into account, as shown in the right panel in Fig. 8 and lower panel in Fig. 10, respectively.

The mechanism of the influence of disorder on the long-range spatial coherence is seen from comparison of the time evolutions of calculated $\psi(x)$, $k_m(x)$ and the interferogram. The laser pulse excites the condensate with $\psi(x, t=0) = const$. At $t > 0$ this equality is disturbed as both $k(x) \neq 0$ in the expanding condensate and LP energy vary with x due to the variation of $n_c(x)$. In MCs with $\nabla E_{LP} = 0$, these effects result in a symmetric change of $\Delta\phi(x)$ with increasing $|x|$ and thereby do not influence the fringe period in the interferogram of direct and mirror images of condensate emission.

The condensate movement in the gradient of E_{LP} disturbs the equality $\phi(x) = \phi(-x)$ as shown in Fig. 9a displaying $\Delta\phi$ calculated for $dE_{LP}/dx = 2$ meV/mm. It shows that the contribution to $\phi(x)$ connected with the gradient of E_{LP} causes a gradual increase of T_{fr} in the interferogram. Thus the observed increase in T_{fr} in the measured interferograms (Figs. 1 and 2) is well explained

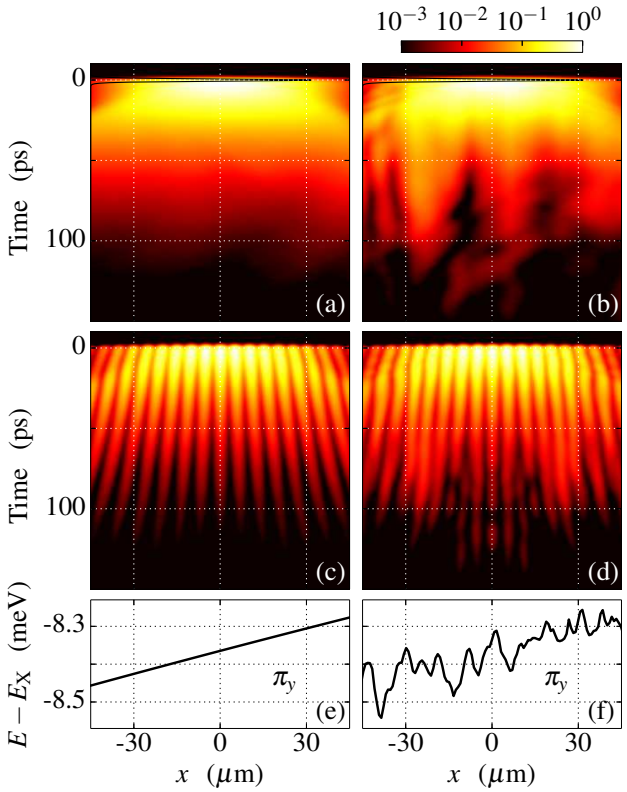

FIG. 8. (Color online) Time dependences of spatial distributions of emission intensity of LP condensate mode excited resonantly with 1.5-ps long pulses $I(x,t)$ (a,b) and interferograms of their direct and mirror images (c,d) calculated for the MC with $\nabla E_{LP}(x) = 2$ meV/mm. The left and right panels show dependences for MCs without and with disorder, respectively. The corresponding dependences $E_{LP}(x)$ are shown in (e) and (f), respectively.

by the occurrence of potential gradient in the investigated wedged MC.

To explain the fluctuations of the fringe period and the appearance of the fork-like structure in the interferogram in #2 the disorder should be taken into consideration. The time evolutions of the interferogram, $\Delta\phi(x)$ at $|x| \leq 15$ μm and $I(k_x)$ at $x = 0$ and ± 15 μm calculated under an assumption that the disorder causes random fluctuations in $E_{LP}(x)$ of 0.1 meV are shown in Figs. 8d, 9b, and the lower panel in Fig. 10, respectively. It is seen that both the fluctuations in $\Delta\phi(x)$ and k_m, and interferogram blurring become well pronounced only at $t \gtrsim 60$ ps when the resonance energy lowers into the region of E_{LP} fluctuations. These correlations show unambiguously that it is the violation of the radial spreading of the condensate that causes the local fluctuations of $\phi(x,t)$ and results in interferogram blurring. The formation of vortices observed in the experiment is also reproduced qualitatively in the simulations of the phase for the condensate spreading in the disordered potential. In particular, Fig. 9b shows that in the simulations the vortex appears at $t \sim 70$ ps, $x = -11$ μm.

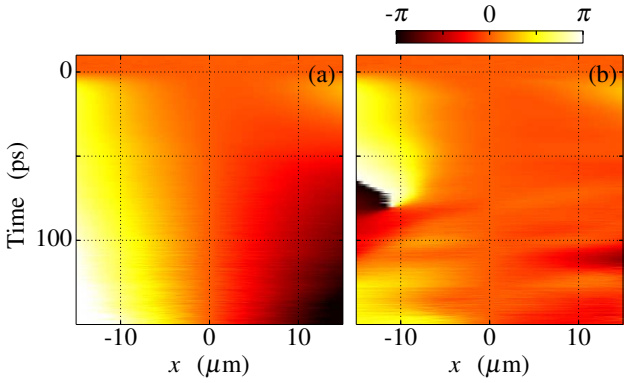

FIG. 9. (Color online) Time dependences of the condensate phase $\Delta\psi(x,t)$ in the MC with $\nabla E_{LP}(x) = 2$ meV/mm without (a) and with (b) disorder. The $E_{LP}(x)$ dependences are shown in Figs. 8e and f, respectively.

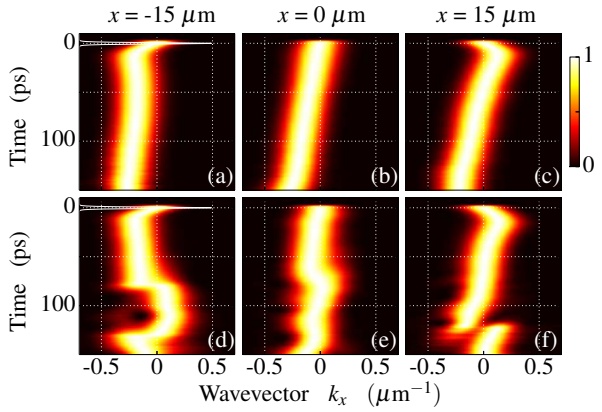

FIG. 10. (Color online) Time evolutions of $|\psi(k)|^2$ in condensate at $x = 0$ and ± 15 μm calculated for MCs with $\nabla E_{LP}(x) = 2$ meV/mm in the absence (upper panel) and presence (lower panel) of the disorder.

Finally, it is of interest to compare the experimental dependencies $g^{(1)}(x,t)$ with calculated ones. For correct comparison the latter are extracted from the interferograms calculated with the same set of parameters as measured ones, namely, the spatial resolution $\delta_x = 2$ μm, $T_{fr} = 7.5$ μm, and $\alpha|\psi^2| = 0.4$ meV. The calculated dependences $g^{(1)}(t)$ for several x_i are shown in Fig. 11. The comparison of these dependences with the experimental ones in Fig. 3d shows that the calculations reproduce qualitatively the main features, namely, a very slow decrease in $g^{(1)}(x_i, -x_i)$ at $t \lesssim 50$ ps when the LP density is sufficiently high to screen potential fluctuations and an oscillating-like decrease in $g^{(1)}$ at larger t when the screening becomes partial.

The quantitative difference in the calculated and experimental values of $g^{(1)}(\Delta x)$ at $t \lesssim 50$ ps is relatively small: the calculated values of $g^{(1)}$ at $x < d$ are in the range 0.85 ± 0.05 whereas the experimental ones in #2 are less by ~ 0.15. We suggest that this difference can be related to the effect of phonons (the experiment was carried out at $T = 10$ K) and/or rest carriers in the QWs neglected in the calculations as both the experiment and calculations show a very weak dependence of $g^{(1)}(\Delta x)$ on the amplitude of E_{LP} fluctuations at high condensate densities.

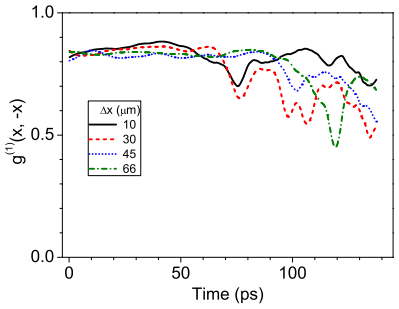

FIG. 11. (Color online) Calculated dependence of $g^{(1)}(\Delta x, t)$ in the resonantly excited condensate in the MC with $\nabla E_{LP}(x) = 2$ meV/mm in the presence of the disorder obtained from interferograms calculated for the spatial resolution $\delta_x = 2$ μm with $T_{fr} = 7.5$ μm.

IV. CONCLUSION

We have investigated time evolution of long-range spatial coherence in a freely decaying exciton-polariton condensate in high Q GaAs MCs with LP lifetime of 20-25 ps excited at the normal to its plane. Resonant excitation with picosecond pump pulses leaves the exciton reservoir empty which enables to realize a very high long-range spatial coherence in the condensate. The comparison of $g^{(1)}$ in the condensates excited resonantly and nonresonantly in the same sample showed that the main reason for a much smaller L_c in the nonresonantly excited condensate is its interaction with the exciton reservoir.

In the absence of the exciton reservoir, the condensate expansion caused by the repulsive LP-LP interaction and its movement in the gradient of E_{LP} have a strong influence on its time evolution in the real and momentum spaces but have little effect on its spatial coherence that persists during tens of ps when n_c decreases by more than an order of magnitude.

The disorder is found to lead to strong local fluctuations of the condensate phase and vortex formation only when the interaction energy becomes smaller than the amplitude of fluctuations in $E_{LP}(x)$. In this case the redistribution of polariton fluxes in the condensate leads to local short time phase fluctuations that, in turn, result in a local variation of the condensate emission direction, on the one hand, and an oscillating-like decrease in $g^{(1)}(x)$ at large t, on the other hand, but have little effect on the overall coherence.

Both the very weak disturbance of the overall condensate coherence in the excited spot and in the condensate expanding out of it, local short time fluctuations in the condensate phase and disorder-related vortex formation

under the resonant excitation are well reproduced within the framework of Gross-Pitaevskii equations when both the limited size of the pumped spot, the gradient of E_{LP}, and the disorder are taken into account.

ACKNOWLEDGMENTS

We are grateful to M. M. Glazov, S. S. Gavrilov, N. A. Gippius, S. G. Tikhodeev, and V. B. Timofeev for fruitful discussions. The work was supported by the Russian Science Foundation (Grant No. 14-12-01372) and the State of Bavaria.

[1] C. J. Pethick, H. Smith, *Bose-Einstein Condensation in Dilute Gases* (Cambridge University Press, 2008).
[2] S. Ritter, A. Öttl, T. Donner, T. Bourdel, M. Köhl, and T.Esslinger, Phys. Rev. Lett. **98**, 090402 (2007).
[3] J. Kasprzak, M. Richard, S. Kundermann, A. Baas, P. Jeambrun, J.M. J. Keeling, F.M. Marchetti, M.H. Szymańska, R. André, J. L. Staehli, V. Savona, P.B. Littlewood, B. Deveaud, and Le Si Dang, Nature **443**, 409 (2006).
[4] R. Balili, V. Hartwell, D. Snoke, L. Pfeiffer, K. West, Science **316**, 07 (2007).
[5] A. V. Kavokin, J. J. Baumberg, G. Malpuech, F. P. Laussy, *Microcavities* (Oxford University Press, Oxford, 2007).
[6] A. Amo, J. Lefrère, S. Pigeon, C. Adrados, C. Ciuti, I. Carusotto, R. Houdré, E. Giacobino, and A. Bramati, Nat. Phys. **5**, 805 (2009).
[7] K. G. Lagoudakis, M. Wouters, M. Richard, A. Baas, I. Carusotto, R. André, Le Si Dang, and B. Deveaud-Plédran, Nat. Phys. **4**, 706 (2008).
[8] A. V. Larionov, V. D. Kulakovskii, S. Höfling, C. Schneider, L. Worschech, and A. Forchel, Phys. Rev. Lett. **105**, 256401 (2010).
[9] K. G. Lagoudakis, B. Pietka, M. Wouters, R. André, and B. Deveaud-Plédran, Phys. Rev. Lett. **105**, 120403 (2010).
[10] H. Deng, G. S. Solomon, R. Hey, K.H. Ploog, and Y. Yamamoto, Phys. Rev. Lett. **99**, 126403 (2007).
[11] G. Roumpos, M. Lohse, W. H. Nitsche, J. Keeling, M. H. Szymańska, P. B. Littlewood, A. Löffler, S. Höfling, L.Worschech, A. Forchel, and Y. Yamamoto, Proc. Natl. Acad. Sci. USA **109**, 6467 (2012).
[12] G. Nardin, K. G. Lagoudakis, M. Wouters, M. Richard, A. Baas, R. André, Le Si Dang, B. Pietka, and B. Deveaud-Plédran, Phys. Rev. Lett. **103**, 256402 (2009).
[13] H. Ohadi, E. Kammann, T. C. H. Liew, K. G. Lagoudakis, A.V. Kavokin, and P. G. Lagoudakis, Phys. Rev. Lett. **109**, 016404 (2012).
[14] C. W. Lai, N. Y. Kim, S. Utsunomiya, G. Roumpos, H. Deng, M. D. Fraser, T. Byrnes, P. Recher, N. Kumada, T. Fujisawa, and Y. Yamamoto, Nature **450**, 529 (2007).
[15] M. Steger, G. Liu, B. Nelsen, C. Gautham, D. W. Snoke, R. Balili, L. Pfeiffer, and K. West, Phys. Rev. B **88**, 235314 (2013).
[16] V.V. Belykh, N. N. Sibeldin, V. D. Kulakovskii, M. M. Glazov, M. A. Semina, C. Schneider, S. Höfling, M. Kamp, and A. Forchel, Phys. Rev. Lett. **110**, 137402 (2013).
[17] D. A. Mylnikov, V. V. Belykh, N. N. Sibeldin, V. D. Kulakovskii, C. Schneider, S. Höfling, M. Kamp, and A. Forchel JETP. Lett. **101**, 513 (2015).
[18] J. Schmutzler, T. Kazimierczuk, O. Bayraktar, M. Assmann, M. Bayer, S. Brodbeck, M. Kamp, C. Schneider, and S. Höfling, Phys. Rev. B **89**, 115119 (2014).
[19] G. Malpuech, D. D. Solnyshkov, H. Ouerdane, M. M. Glazov, and I. Shelykh, Phys. Rev. Lett. **98**, 206402 (2007).
[20] L.Fontanesi, M. Wouters, and V. Savona, Phys. Rev. Lett. **103**, 030403 (2009).
[21] A. Baas, K. G. Lagoudakis, M. Richard, R. André, Le Si Dang, and B. Deveaud-Plédran, Phys. Rev. Lett. **100**, 170401 (2008).
[22] V. L. Berezinskii, Sov. Phys. JETP **34**, 610 (1972).
[23] J. M. Kosterlitz and D. J. Thouless, J. Phys. C: Solid State Phys. **6**, 1181 (1973).
[24] W. H. Nitsche, Na Young Kim, G. Roumpos, C. Schneider, M. Kamp, S. Höfling, A. Forchel, and Y. Yamamoto, Phys. Rev. B **90**, 205430 (2014).
[25] W. H. Nitsche, N. Y. Kim, G. Roumpos, C. Schneider, S. Höfling, A. Forchel, and Y. Yamamoto, Phys. Rev. A **93**, 053622 (2016).
[26] E. A. Cerda-Méndez, D. N. Krizhanovskii, M. Wouters, R. Bradley, K. Biermann, K. Guda, R. Hey, P.V. Santos, D. Sarkar, and M. S. Skolnick, Phys. Rev. Lett. **105**, 116402 (2010).
[27] M. Thunert, A. Janot, H. Franke, C. Sturm, T. Michalsky, M. D. Martin, L. Viña, B. Rosenow, M. Grundmann, and R. Schmidt-Grund, Phys. Rev. B **93**, 064203 (2016).
[28] S. S. Gavrilov, A. V. Sekretenko, S. I. Novikov, C. Schneider, S. Höfling, M. Kamp, A. Forchel and V. D. Kulakovskii, Appl. Phys. Lett. **102**, 011104 (2013).
[29] S. S. Gavrilov, A. S. Brichkin, S. I. Novikov, S. Höfling, C. Schneider, M. Kamp, A. Forchel, and V. D. Kulakovskii, Phys. Rev. B **90**, 235309 (2014).
[30] S. S. Gavrilov, A. S. Brichkin, Ya. V. Grishina, C. Schneider, S. Höfling, and V. D. Kulakovskii, Phys. Rev. B **92**, 205312 (2015).
[31] The thin MC layer consisted from GaAs and AlAs layers on a GaAs substrate is compressed as it inherits the GaAs lattice parameter. Removing the substrate in a limited area leads to inhomogeneous lateral deformation of the MC layer in this region (the layer becomes convex). The large difference in the lengths of the sides of the etched area ($\sim$ 300x700 μm) results in a difference in the MC strain along the sides of etched area.
[32] O. Penrose and L. Onsager, Phys. Rev. **104**, 576 (1956).
[33] R. J. Glauber, Phys. Rev. **131**, 2766 (1963).
[34] I. A. Shelykh, D. D. Solnyshkov, G. Pavlovic, and G. Malpuech Phys. Rev. B **78**, 041302(R) (2008)
[35] D. N. Krizhanovskii, E. A. Cerda-Méndez, S. Gavrilov, D. Sarkar, K. Guda, R. Bradley, P. V. Santos, R. Hey, K. Biermann, M. Sich, F. Fras, and M. S. Skolnick Phys. Rev. B **87**, 155423 (2013).
[36] A. V. Sekretenko, S. S. Gavrilov, S. I. Novikov, V. D. Kulakovskii, S. Höfling, C. Schneider, M. Kamp, and A.

Forchel, Phys. Rev. B **88**, 205302 (2013).

[37] S. S. Gavrilov, A. A. Demenev, V. D. Kulakovskii, JETP Lett. **100**, 817 (2015).